Authors response to AMT 2022-906 Initial Referee Report

We deeply appreciate the time and effort the initial referee dedicated to providing valuable feedback towards helping us improve the manuscript. We have been able to incorporate changes to reflect most of the suggestions provided by the referee in our manuscript.
The referee comments/suggestions are in black, and our responses are in red, the listed page numbers refer to the lines of the manuscript where the new corrections are observed.

This manuscript suggests an interesting approach of measuring virga and the potential connection of virga with particulate matter concentrations at the surface using ceilometers and in conjunction with other supporting measurements.

Thank you for your comment.

Table 1 and other results throughout the manuscript could potentially be strengthened using 5-minute TCEQ CAMS data rather than the hourly averaged data. The 5-minute CAMS data is available upon request from TCEQ.

The 50 virga episodes that were classified in this work are unevenly distributed throughout the study period of 7 years. Since the 5-minute data was not available to us we decided to use the one-hour average data which is readily available in the public domain. We are grateful for your suggestion and will seek the 5-minute data for future use.

Include wind data on the Skew-T plots.

The existing Skew-T plots (Figure 3, 6(b), and 8(b)) have been modified to include wind data.

An all-sky fisheye camera colocated with the ceilometer saving an image everyone or five minutes could help with the verification of virga events and instances of dry microbursts.

That is a very good suggestion. We will implement it in near future, based on the availability of funds.

It is not clear that a wind gust in the absence of surface precipitation during what may be a period of a ceilometer-verified virga event is an indication of a dry microburst. It is consistent but inconclusive.

Ceilometer provides the columnar aerosol backscatter profile and based on that it successfully identified virga precipitation. Dry microbursts are defined by (Fujita, 1981 and Wakimoto, 1985) as convectively driven small downdrafts of less than 4 km in outflow diameter accompanied by little or no rain between the beginning and the end of the intense winds for a short duration of time. They are commonly associated with virga or precipitation that evaporates before reaching the ground.

Since we observed a substantial increase in the surface measured maximum wind gusts during the virga event, we attributed these horizontal winds to dry microburst. Of course, we also agree that more sophisticated remote sensing instrumentation, such as radio wind profiler or wind lidars, at the site could be helpful in providing more information on vertical winds such as to capture the downbursts. Ours represent the first study of virga events for our region. It is our hope that the publication of this manuscript will create an incentive to pursue these types of studies, which are particularly important in severe dry regions, such as ours.

Fujita, T. T. (1981). Tornadoes and Downbursts in the Context of Generalized Planetary Scales, Journal of Atmospheric Sciences, 38(8), 1511-1534. Retrieved Dec 19, 2022, from
https://journals.ametsoc.org/view/journals/atsc/38/8/1520-0469_1981_038_1511_taditc_2_0_co_2.xml

Wakimoto, R. M. (1985). Forecasting Dry Microburst Activity over the High Plains, Monthly Weather Review, 113(7), 1131-1143. Retrieved Dec 19, 2022, from https://journals.ametsoc.org/view/journals/mwre/113/7/1520-0493_1985_113_1131_fdmaot_2_0_co_2.xml

The non-columnar Case Study 2 potential virga event on 10 March 2019 needs further explanation on the timing and the lack of a surface level PM enhancement.

This is an excellent point raised by the reviewer. We would like to use both the cases discussed in this paper to present a convincing justification. In addition, the following modification and explanation are added to the respective sections of the manuscript as well.
For uniformity and convenience of our readers, we have all the figures in UTC and figures 6 and 8 (a), (c) and (d) have a uniform y-axis scale respectively. Additionally, we have added markers for radiosonde data availability (dashed lines) and highlighted portion to emphasize the section of the figure under examination. We hope this will help convey our explanation to the reviewers and readers more effectively.

Line 265-290: Following modifications/addition made.

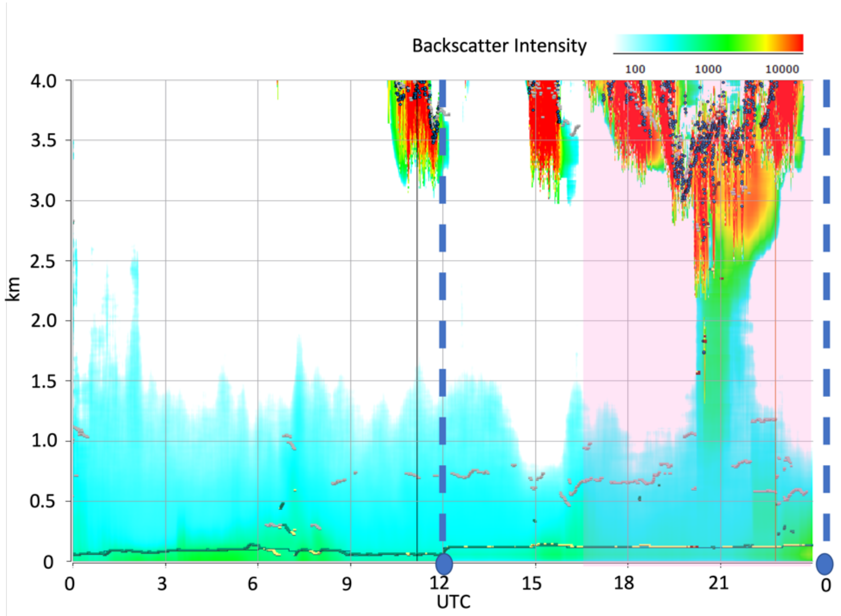

Figure 5: Virga event from 31 March 2015 (shaded region), when a columnar aerosol profile can be seen between around 20-22 UTC reaching the surface aerosol layer. The blue dashed lines and circles indicate availability of radiosonde data.

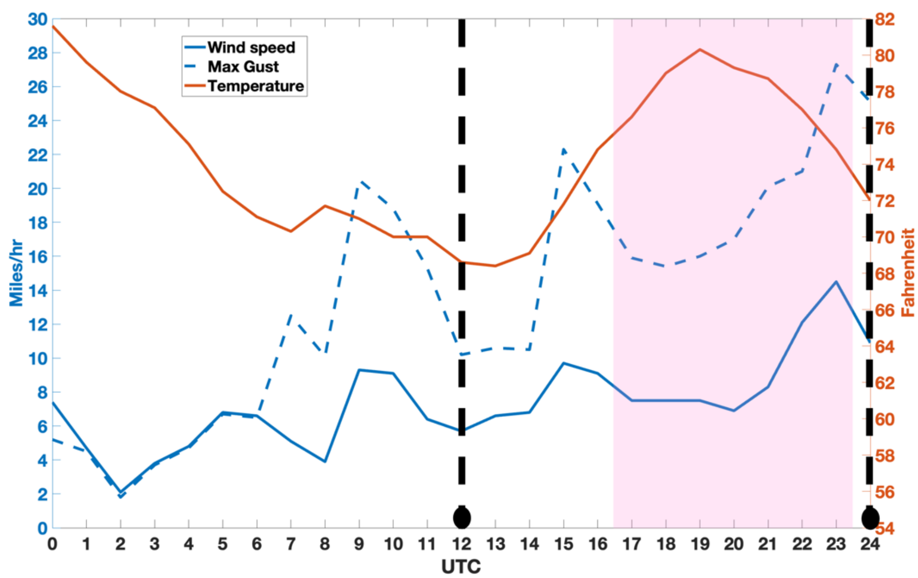

(a)

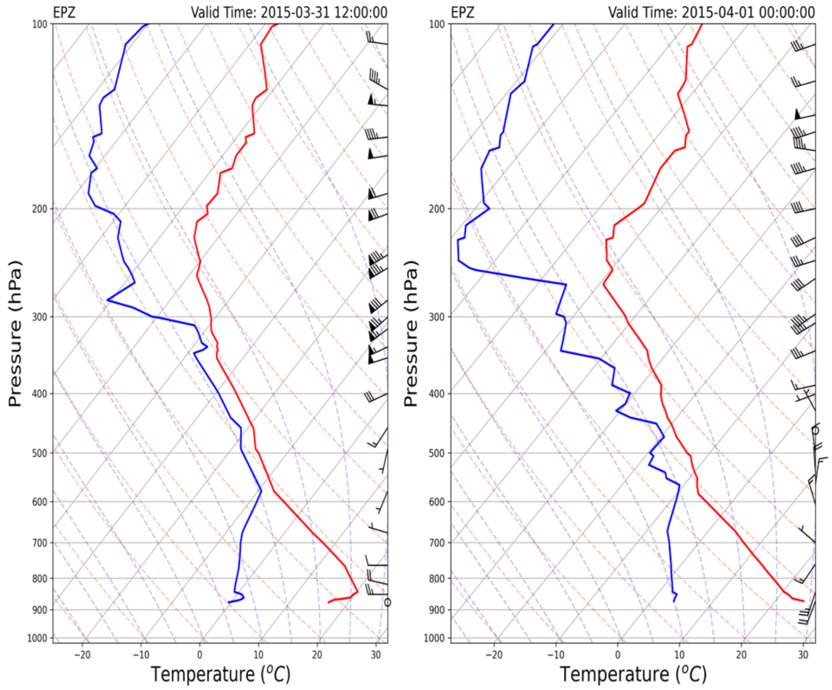
EPZ
Valid Time: 2015-03-31 12:00:00
Pressure (hPa)
Temperature (°C)
EPZ
Valid Time: 2015-04-01 00:00:00
Pressure (hPa)
Temperature (°C)

(b)

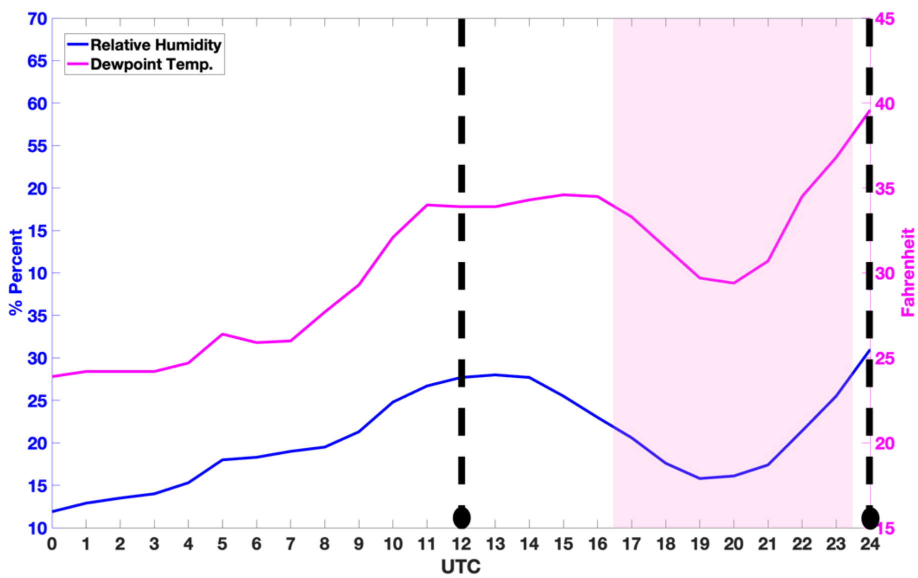
Relative Humidity
Dewpoint Temp.
% Percent
Fahrenheit
UTC

(c)

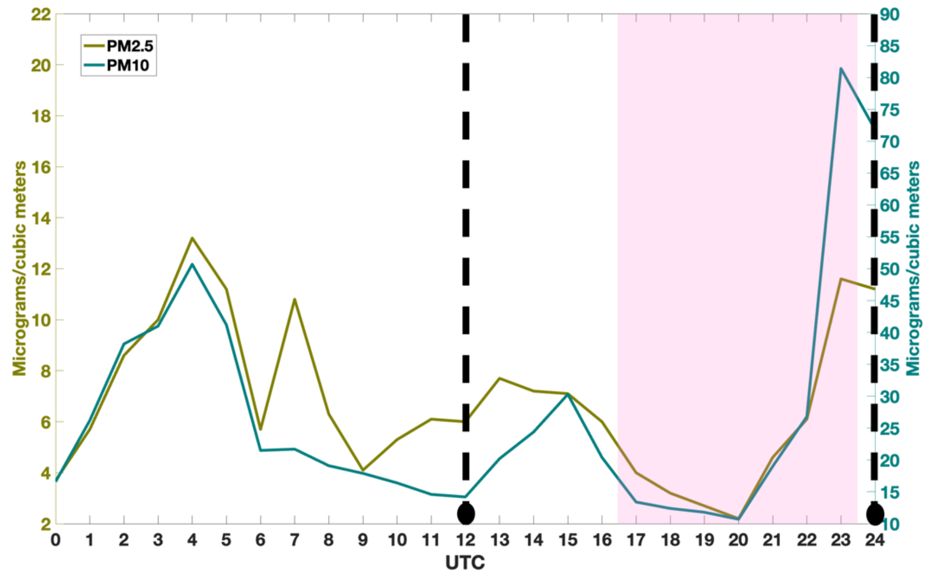

(d)

Figure 6: Hourly measurements from TCEQ CAMS 12 UTEP for 31 March 2015, (a) wind speed (solid blue), maximum wind gust (dotted blue) in miles/hr and surface temperature (red) in Fahrenheit; (b) sounding along with wind barbs from NWS for 31 March 2015 12 UTC and 1 April 2015 00 UTC (T_d: blue, T:red); (c) relative humidity (purple) and dewpoint temperature (pink); (d) PM2.5 concentration (olive) and PM10 concentration (teal). Shaded portions represent virga event and black dashed lines, and dots represent availability of radiosonde data.

Figure 6a shows an increase in surface wind speed and maximum gust during the virga event (shaded). The daytime temperature peaks at 19 UTC and then begins to fall. The radiosonde vertical profiles on 31 March 2015 at 12 UTC and 1 April 2015 at 0 UTC provide a better understanding of the thermodynamic state of the atmosphere within and above the boundary layer (Figure 6b). Temperature (red) and dew point temperature (blue) are further apart between 876 mb (1.3 km above sea level, a.s.l.) and 577 mb (4.7 km a.s.l.), indicating lower relative humidity at these levels. In the 0 UTC sounding, we observe the temperature drifting from the adiabatic ascent curve showing a diabatic behavior. This loss of latent heat energy of the air parcel can be attributed to the air column which has cooled down after the evaporation of precipitation underneath the clouds. Another important piece of information we obtain from the soundings is the wind intensity near the surface. As seen in the wind barbs associated with the 12 and 0 UTC sounding, winds are calm between 732 mb (2.7 km a.s.l.) and 655 mb (3.7 km a.s.l.). However, near the surface we observe strong winds (around 23-34 mph) which appears to be decoupled from winds between the cloud base and the surface. Based on the thermodynamic and meteorological evidence, it can be concluded that virga in case 1 was intense in nature.

Line 320-345: following modifications/addition made.

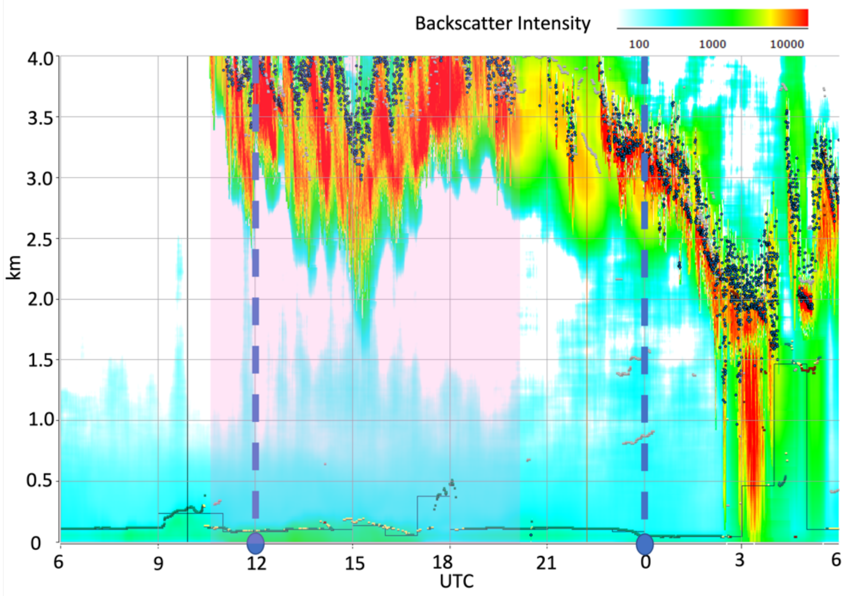

Figure 7: Virga event from 10-11 March 2019 (shaded region), starting from 10:30-20 UTC, light precipitation can also be observed between 3-4 UTC.

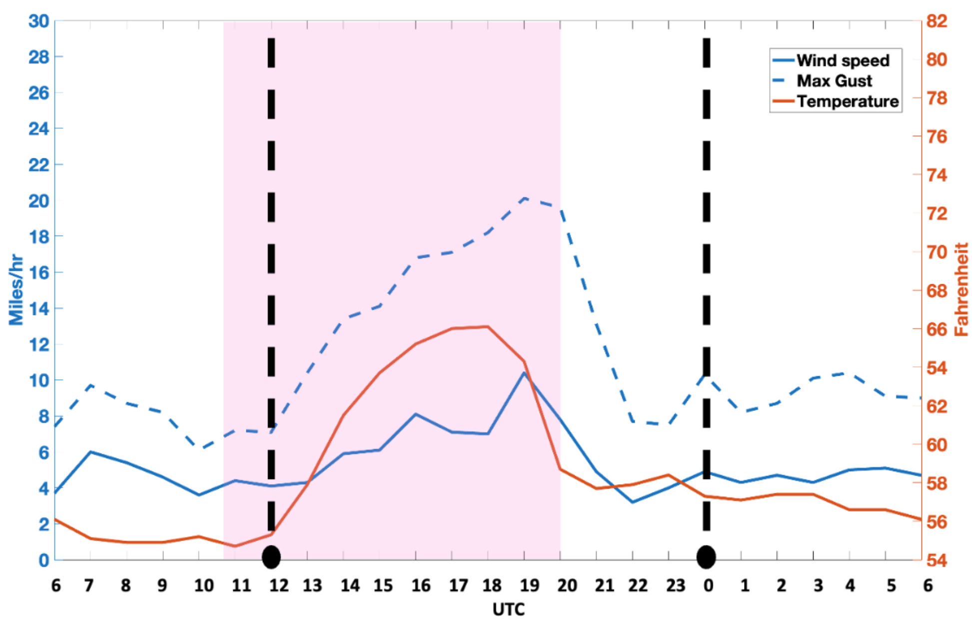

(a)

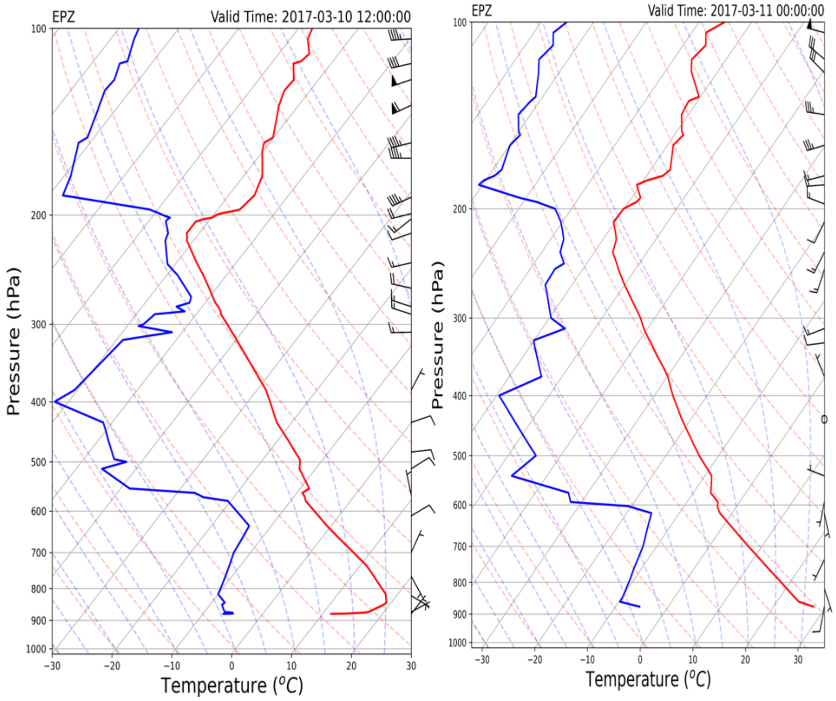
EPZ
Valid Time: 2017-03-10 12:00:00
Pressure (hPa)
Temperature (^oC)
EPZ
Valid Time: 2017-03-11 00:00:00
Pressure (hPa)
Temperature (^oC)

(b)

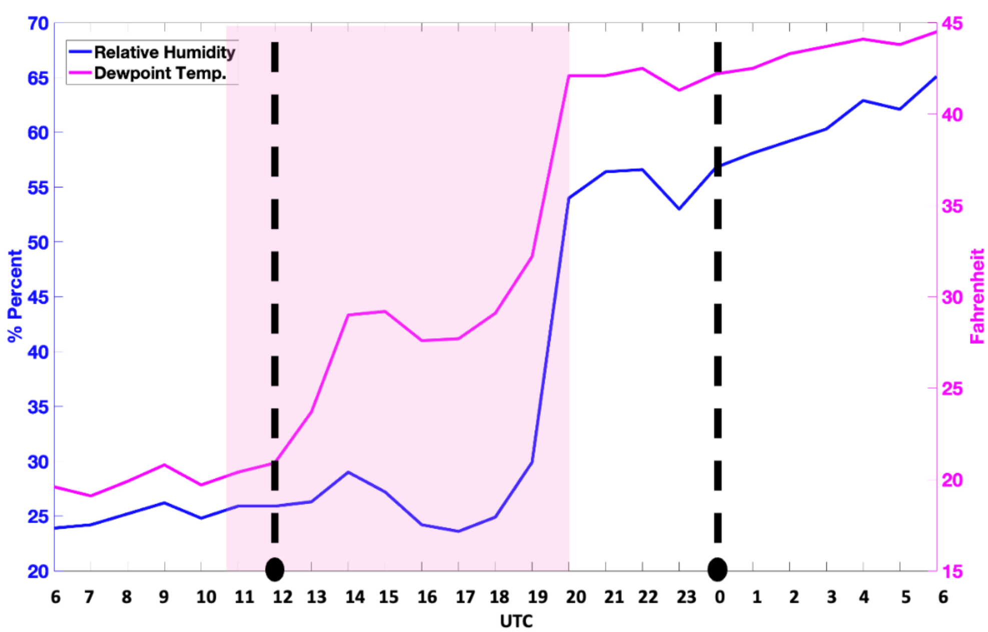
Relative Humidity
Dewpoint Temp.
% Percent
Fahrenheit
UTC

(c)

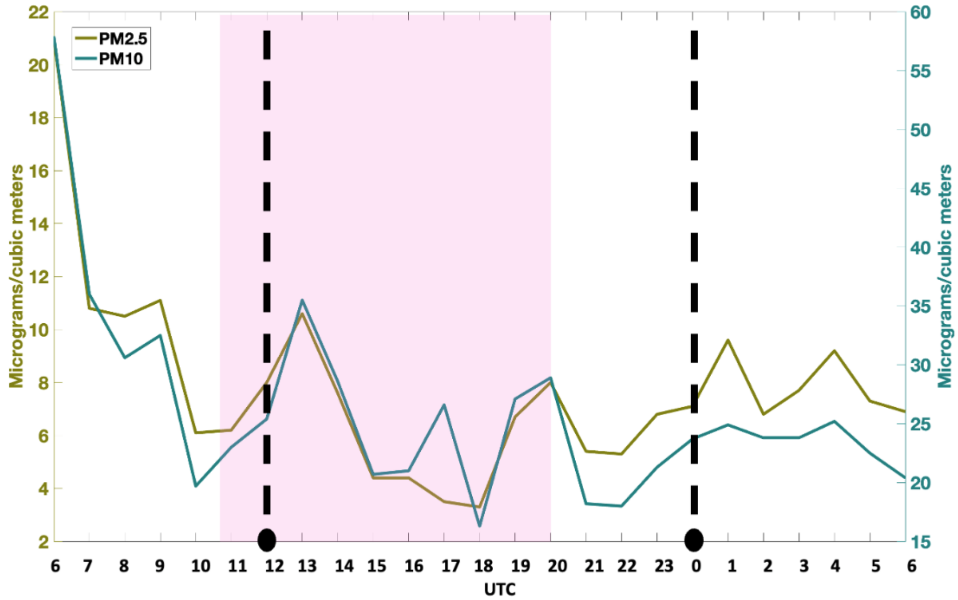

(d)

Figure 8: Hourly surface measurements in UTC from CAMS 12 UTEP for 10-11 March 2019, (a) wind speed (solid blue), maximum wind gust (dotted blue) in miles/hr and surface temperature (red) in Fahrenheit; (b) sounding along with wind barbs from NWS for 10 March 2017 12 UTC and 11 March 2017 00 UTC (T_d: blue, T:red); (c) relative humidity (purple) and dewpoint temperature (pink); (d) $PM_{2.5}$ concentration (olive) and PM_{10} concentration (teal). Shaded portions represent the virga event and black dashed lines, and dots represent availability of radiosonde data.

The radiosonde vertical profiles reveal the absence of strong winds on the surface and within the boundary layer in the case of non-columnar virga. The 12 UTC profile overlaps with the virga's initial phase, whereas the 0 UTC profile provides information after the virga has ended (figure 8b). Both soundings indicate the presence of dry layers between 900 and 600 mb and 600 and 300 mb, respectively. In contrast to the columnar virga, the temperature profile at 0 UTC follows the adiabatic ascent curve between 880 to 600 mb. Figure 8a shows that the surface wind and gust intensity were lower than what was observed in the columnar case. Based on ground measurements, we can see in figure 8 c that the surface was relatively more humid than in the columnar case and that the percent relative humidity increased rapidly at the end of the virga event. Based on the evidence presented above, we hypothesize that the virga intensity was lower in the non-columnar case, resulting in mild winds at the surface and as shown in figure 8d, hence relatively lower concentrations of fine aerosol loading into the atmosphere. Furthermore, the higher moisture content in the air resulted in lower PM concentrations.

The paper is worthy of review, and upon making revisions, has potential for publication in AMT.

Thank you for your valuable comments and suggestions. It helped us enhance the content of the manuscript.